

Creative Commons Attribution 4.0 International (CC BY 4.0)

<https://creativecommons.org/licenses/by/4.0/>

Access to this work was provided by the University of Maryland, Baltimore County (UMBC) ScholarWorks@UMBC digital repository on the Maryland Shared Open Access (MD-SOAR) platform.

**Please provide feedback**

Please support the ScholarWorks@UMBC repository by emailing [scholarworks-group@umbc.edu](mailto:scholarworks-group@umbc.edu) and telling us what having access to this work means to you and why it's important to you. Thank you.

LETTER • OPEN ACCESS

## Greater aridity increases the magnitude of urban nighttime vegetation-derived air cooling

To cite this article: Peter C Ibsen *et al* 2021 *Environ. Res. Lett.* **16** 034011

View the [article online](#) for updates and enhancements.

You may also like

- [Global assessment of urban trees' cooling efficiency based on satellite observations](#)  
Qiquan Yang, Xin Huang, Xiaohua Tong et al.
- [European Extremely Large Telescope Site Characterization III: Ground Meteorology](#)  
Antonia M. Varela, Héctor Vázquez Ramió, Jean Vernin et al.
- [Substantial increase in daytime-nighttime compound heat waves and associated population exposure in China projected by the CMIP6 multimodel ensemble](#)  
Wenxin Xie, Botao Zhou, Zhenyu Han et al.

ENVIRONMENTAL RESEARCH  
LETTERS

## LETTER

Greater aridity increases the magnitude of urban nighttime  
vegetation-derived air cooling

## OPEN ACCESS

RECEIVED  
14 October 2020REVISED  
21 January 2021ACCEPTED FOR PUBLICATION  
25 January 2021PUBLISHED  
15 February 2021

Original content from  
this work may be used  
under the terms of the  
[Creative Commons  
Attribution 4.0 licence](#).

Any further distribution  
of this work must  
maintain attribution to  
the author(s) and the title  
of the work, journal  
citation and DOI.



Peter C Ibsen<sup>1</sup> , Dorothy Borowy<sup>2</sup>, Tyler Dell<sup>3</sup>, Hattie Greydanus<sup>4</sup>, Neha Gupta<sup>5</sup>, David M Hondula<sup>6</sup> , Thomas Meixner<sup>5</sup>, Mary V Santelmann<sup>4</sup>, Sheri A Shiflett<sup>7</sup>, Michael C Sukop<sup>8</sup>, Christopher M Swan<sup>2</sup>, Michelle L Talal<sup>4</sup> , Miguel Valencia<sup>8</sup>, Mary K Wright<sup>6</sup> and G Darrel Jenerette<sup>1,9</sup>

<sup>1</sup> Department of Botany and Plant Sciences, University of California Riverside, Riverside, CA 92507, United States of America

<sup>2</sup> Department of Geography and Environmental Systems, University of Maryland Baltimore County, Baltimore, MD 21250, United States of America

<sup>3</sup> Civil and Environmental Engineering, Colorado State University, Fort Collins, CO 80523, United States of America

<sup>4</sup> College of Earth, Ocean, and Atmospheric Sciences, Oregon State University, Corvallis, OR 97331, United States of America

<sup>5</sup> Hydrology and Atmospheric Sciences, The University of Arizona, Tucson, AZ 85721, United States of America

<sup>6</sup> School of Geographical Sciences and Urban Planning, Arizona State University, Tempe, AZ 85287, United States of America

<sup>7</sup> Environmental Sciences, University of North Carolina Wilmington, Wilmington, NC 28403, United States of America

<sup>8</sup> Department of Earth and Environment, Florida International University, Miami, FL 33199, United States of America

<sup>9</sup> Center for Conservation Biology, University of California Riverside, Riverside, CA 92507, United States of America

E-mail: [pibse001@ucr.edu](mailto:pibse001@ucr.edu)

**Keywords:** urban heat, vegetation cooling, ecosystem service, aridity, air temperature

Supplementary material for this article is available [online](#)

**Abstract**

High nighttime urban air temperatures increase health risks and economic vulnerability of people globally. While recent studies have highlighted nighttime heat mitigation effects of urban vegetation, the magnitude and variability of vegetation-derived urban nighttime cooling differs greatly among cities. We hypothesize that urban vegetation-derived nighttime air cooling is driven by vegetation density whose effect is regulated by aridity through increasing transpiration. We test this hypothesis by deploying microclimate sensors across eight United States cities and investigating relationships of nighttime air temperature and urban vegetation throughout a summer season. Urban vegetation decreased nighttime air temperature in all cities. Vegetation cooling magnitudes increased as a function of aridity, resulting in the lowest cooling magnitude of 1.4 °C in the most humid city, Miami, FL, and 5.6 °C in the most arid city, Las Vegas, NV. Consistent with the differences among cities, the cooling effect increased during heat waves in all cities. For cities that experience a summer monsoon, Phoenix and Tucson, AZ, the cooling magnitude was larger during the more arid pre-monsoon season than during the more humid monsoon period. Our results place the large differences among previous measurements of vegetation nighttime urban cooling into a coherent physiological framework dependent on plant transpiration. This work informs urban heat risk planning by providing a framework for using urban vegetation as an environmental justice tool and can help identify where and when urban vegetation has the largest effect on mitigating nighttime temperatures.

**1. Introduction**

Average nighttime air temperatures ( $T_{\text{air}}$ ) have been steadily increasing across the US in recent years, with implications for reduced human health and well-being [1, 2]. Rising nighttime  $T_{\text{air}}$  is especially important for heat vulnerability during summer months when heat waves intensify heat-related health effects, and are also a major global cause of weather-related mortality [3–5]. Urbanization exacerbates  $T_{\text{air}}$

increases through the urban heat island (UHI) effect, which describes how nighttime  $T_{\text{air}}$  in cities increases relative to non-urban locations through increased daytime heat storage [6]. With increasing urbanization, more people are becoming vulnerable to inequitable distributions of heat risk and increased cooling costs [7, 8]. Within cities, developed areas with little vegetation result in hot spots where local temperatures are substantially greater than the city-wide average, exacerbating UHI effects [9–11]. Not

only does urban warming elevate health risks, high temperatures also increase energy costs due to air conditioning [8, 12]. While a variety of aspects of urban form can influence urban temperatures such as cool pavements, green roofs, and urban wetlands [13, 14], the cooling capacity of urban vegetation may be a key factor determining the health and well-being of a neighborhood [15]. Increasing urban vegetation density has been proposed as an adaptation approach for mitigating urban nighttime temperatures and resulting heat-related vulnerabilities [16–18]. However, recent work has revealed substantial variability in the magnitude of vegetation-derived nighttime cooling (Delta  $T_{veg}$ ). In Madison, WI, recent work showed only 1 °C air cooling associated with urban vegetation, while studies in Los Angeles and Palm Springs, CA, reported a mean 2.5 °C and 4.9 °C Delta  $T_{veg}$ , respectively [9, 17, 19]. In Salt Lake City, UT, nighttime Delta  $T_{veg}$  in vegetated parks reached up to 3.3 °C [20]. A more comprehensive evaluation of Delta  $T_{veg}$  is needed, both within and among cities.

Variability in vegetation-derived cooling may reflect multiple physiological mechanisms responsible for air-cooling effects. Urban cooling can occur through shading and by transpiration, both of which alter the urban energy balance by moderating sensible and latent heat fluxes [21–23]. While atmospheric factors such as irradiance intensity and windspeed also influence latent and sensible heat flux [24–26], the positive effect of atmospheric aridity on transpiration indicates that humidity and temperature may influence energy dynamics [27, 28]. Atmospheric aridity can be measured as the vapor pressure deficit (VPD), which describes the difference between the amount of water pressure the atmosphere can hold (saturation vapor pressure) and the total amount of water pressure at a specific temperature (actual water vapor pressure) [29]. Transpiration reduces heat by increasing latent heat flux as energy is used to evaporate water from leaves [6]. While vegetation rooted in dry soils can limit water loss by closing leaf stomata, transpiration from urban vegetation can be maintained even in high heat and aridity because regular irrigation mitigates physiological responses to water limitation [27, 30]. In both urban and natural settings, the tight coupling of VPD and plant transpiration has been well established [31, 32], as are the positive correlations between VPD and Delta  $T_{veg}$  within certain cities [33, 34]. However, the direct linking of VPD at the air cooling potential of urban vegetation has not been shown across multiple cities of varying climates and mean summer VPD values.

While Delta  $T_{veg}$  exhibits a relationship with VPD, the high variation among results of prior studies investigating urban Delta  $T_{veg}$  in different climate regions reveals a gap in our understanding of key drivers for the cooling capacity of urban vegetation [9, 17]. To reconcile differences among the estimated Delta  $T_{veg}$ , we ask, how does the magnitude of

vegetation-derived cooling vary within and among cities of the United States? We hypothesize that Delta  $T_{veg}$  is predominantly affected by VPD and other atmospheric processes that influence vegetation transpiration.

We test this transpiration hypothesis by measuring the variation of nighttime  $T_{air}$  across a vegetation gradient within and among cities representing a range of aridity. By using a novel network of microclimate sensors in eight U.S. cities, we predict that daytime VPD, windspeed, and solar irradiance will be positively correlated with Delta  $T_{veg}$ , with daytime VPD having the strongest effect. Among cities, we anticipate that Delta  $T_{veg}$  will be greater in cities with higher VPD, and within cities we predict great Delta  $T_{veg}$  during weather patterns that increase aridity. The high temporal resolution, spatial extent, and seasonal extent of the sensor networks provided opportunities to observe heat wave events in each city and temporal shifts in local climates such as heat waves and monsoons, which allowed multiple tests of predictions on the importance of atmospheric drivers of transpiration influencing the magnitude of Delta  $T_{veg}$ .

## 2. Methods

### 2.1. Study sites

Our study took place within eight major U.S. cities that span a gradient of aridity from Miami (mean August VPD: 0.67 kPa) to Las Vegas (mean August VPD: 5.86 kPa) (figure 1). Each study city was selected based on metro area populations larger than 1,000,000 people and providing a representation of a continental aridity distributions. Each city exhibited a wide range of vegetation density from urban cores to lush parklands (table 1). Sensor distribution within each city was stratified across a gradient of urban vegetation in each city, which was measured spectrally using the normalized difference vegetation index (NDVI). NDVI is a widely used metric of vegetation and encompasses all photosynthetically active vegetation such as trees, grasses, and shrubs [35]. Sensors were deployed in the core of each metropolitan area and the surrounding environs. The extent of deployment differed slightly for each city. All climate data were derived from the nearest airport weather station through the National Centers for Environmental Information ([www.ncdc.noaa.gov/cdo-web/datatools/lcd](http://www.ncdc.noaa.gov/cdo-web/datatools/lcd)). Across cities, midday VPD ranged from 0.0 kPa to 9.4 kPa, and nighttime cooling magnitude ranged from  $-0.6$  °C/NDVI to 8.3 °C/NDVI.

### 2.2. Data acquisition and sensor deployment

To test the relationship of vegetation cover,  $T_{air}$ , and VPD, we deployed 100 microclimate sensors that logged data at 60 min intervals (Maxim Integrated Products, Inc. iButton Thermocron DS1921 & DS1922L) in each city (100 sensors/city, total 800 sensors). This style of sensor has a history of

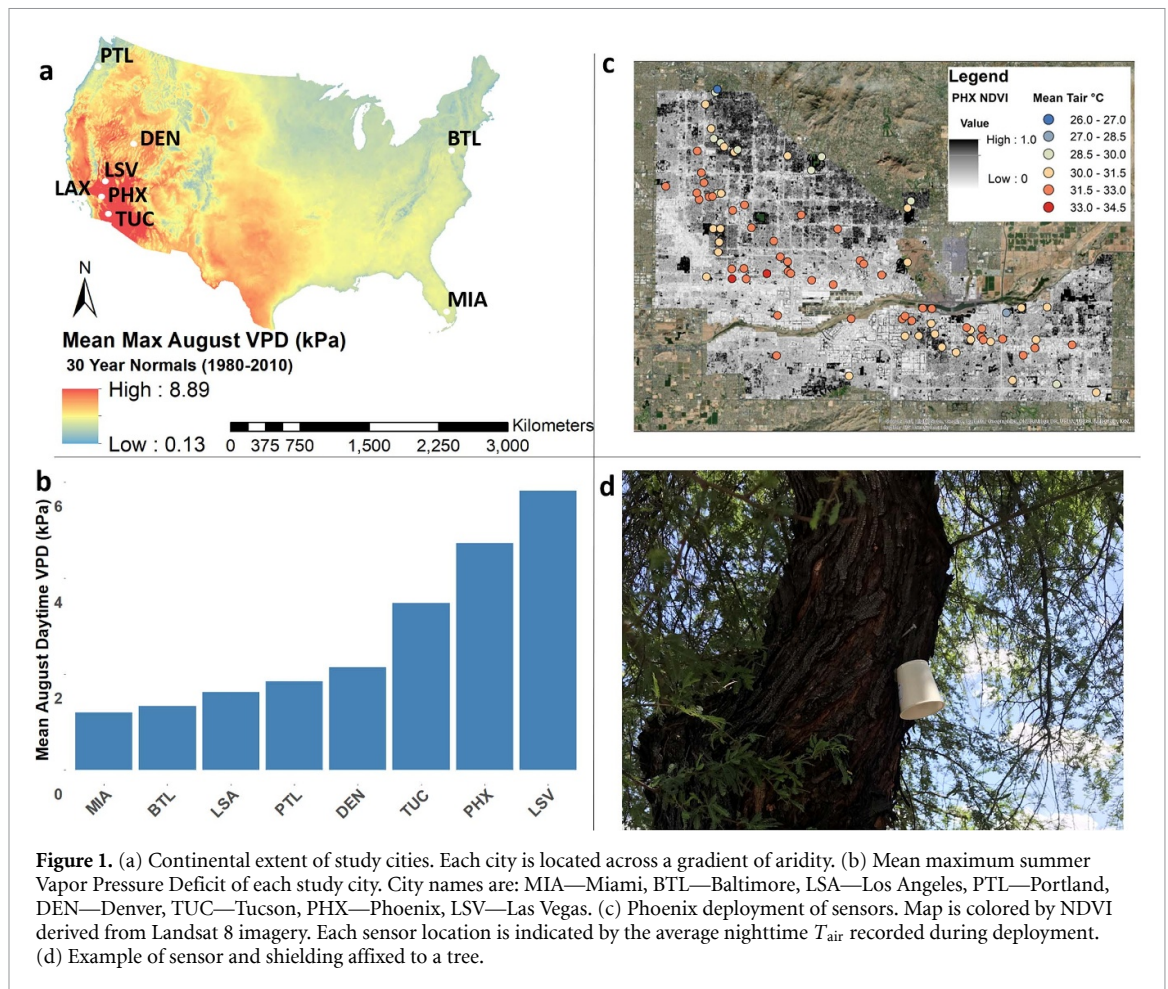


**Figure 1.** (a) Continental extent of study cities. Each city is located across a gradient of aridity. (b) Mean maximum summer Vapor Pressure Deficit of each study city. City names are: MIA—Miami, BTL—Baltimore, LSA—Los Angeles, PTL—Portland, DEN—Denver, TUC—Tucson, PHX—Phoenix, LSV—Las Vegas. (c) Phoenix deployment of sensors. Map is colored by NDVI derived from Landsat 8 imagery. Each sensor location is indicated by the average nighttime  $T_{\text{air}}$  recorded during deployment. (d) Example of sensor and shielding affixed to a tree.

being used for rural and urban microclimate analyses [9, 36, 37]. Each sensor was shielded from direct solar radiation in the manner of Crum *et al* (2017), encased in a breathable mesh and housed in custom polystyrene cylindrical white cups [17]. While the precision ( $\pm 1^\circ\text{C}$ ) of iButtons is coarser than a more commonly used instruments such as Campbell Scientific HMP60-L ( $\pm 0.6^\circ\text{C}$ ), to assess the potential discrepancy in our sensors, we validated our sensors for bias and sensitivity against an HMP60-L sensor (see supplementary appendix for more detail). The low cost of iButtons allowed for a large spatial distribution within and among cities throughout the United States to create a continental scale network of city-scale networks collecting *in-situ* data.

We determined values of NDVI with Landsat 8 imagery of each study city, retrieved for cloud-free days during the study period. Using NDVI as our metric of urban vegetation allowed for the required broader comparisons of within and among city cooling, as NDVI quantifies the variety of vegetation found at the continental scale. NDVI was calculated with Landsat 8 bands 4 (Near Infrared) and 5 (Red), using the equation  $\text{NDVI} = (\text{Band 5} - \text{Band 4}) / (\text{Band 5} + \text{Band 4})$  in the Raster Calculator function of ESRI ArcGIS 10.6.1. We used the aggregate function of the Spatial Analyst extension in ESRI ArcMap to

scale the native Landsat 8 resolution of 30 m per pixel to a coarser 90 m per pixel, which has been identified as an appropriate spatial scale to observe the signal of vegetation induced cooling [19, 38]. Sensors recorded  $T_{\text{air}}$  and relative humidity every hour of every night during summer months in one year (i.e. ~June through September, varying slightly for each deployment) (table 1). The exact time of deployment varied by city, but was between early to late June with sensors recovered in late August to early September (table 1). Locations of sensor deployment were determined by randomly selecting 20 locations within five binned categories of NDVI values spanning the range of NDVI within each city. Binning the distribution of sensors allowed us to capture the full NDVI gradient within each city while also randomizing the sensor placement. Random selection of sites was conducted using the ArcGIS extension Sampling Tool 10 [39], and potential deployment locations were derived as the global positioning system coordinates in the center of a single 90 m pixel [17, 19]. Deployments occurred in 2017, 2018, and 2019. Deployments in each city took approximately 3–5 d, where potential sites for each sensor were located and sensors were affixed to the nearest tree with a full canopy. Sensors were affixed at  $\sim 2$  m height from the surface, and the location was recorded. For areas

**Table 1.** Metadata for each study city. Including population, Koppen Climate Classification, mean summer VPD, range of NDVI (max pixel NDVI – min pixel NDVI) for city extent, the area of each city covered by our recovered sensors, the number of sensors recovered from initial deployment of 100 and dates of sensor deployment.

City	Population (millions of people)	Climate (Koppen)	Mean max august VPD (kPa)	NDVI range (NDVImax – NDVImin)	Sensor deployment area (km <sup>2</sup> )	Sensors recovered (out of 100)	Dates of deployment
Baltimore, MD	2.7	Humid subtropical (Cfa)	1.66	0.788	173.48	78	11 July 2017–30 September 2017
Denver, CO	2.9	Humid continental hot summers with year around precipitation (Dfa)/cold semi-arid climate (BSk)	2.94	0.685	322.42	68	10 July 2018–12 September 2018
Las Vegas, NV	2.2	Hot desert (BWh)	6.32	0.732	360.36	81	11 June 2018–19 August 2018
Los Angeles, CA	13.1	Warm summer mediterranean (CSb)	1.76	0.558	167.90	89	23 June 2017–14 September 2017
Miami, FL	6.1	Tropical monsoon (Am)	1.49	0.657	368.21	80	01 July 18–17 September 2018
Phoenix, AZ	4.8	Hot desert (BWh)	5.71	0.582	277.10	83	15 June 2017–15 August 2017
Portland, OR	2.4	Warm-summer mediterranean climate (Csb)	2.69	0.892	194.76	95	20 June 2017–24 August 2017
Tucson, AR	1.0	Hot semi-arid (BSH)	4.6	0.737	237.37	83	14 June 2019–07 September 2019

in which no suitable tree location could be found near the randomized point, the next nearest location with a similar vegetation density was used. To reduce shading and reflected radiation from nearby structures, trees located next to buildings were not used as sensor sites. Across all cities, ~18% of sensors were lost due to equipment error and/or vandalization.

### 2.3. Data analysis

Data were downloaded from each sensor and restricted to measurements recorded at 01:00 local time, which was approximately five hours past sunset when UHI effects are estimated to be strongest [6]. To assess vegetation's influence on  $T_{\text{air}}$ , we first spatially detrended  $T_{\text{air}}$  patterns within each city of the study. This procedure was needed to remove temperature variation associated with geographic factors such as maritime effects in Los Angeles and Baltimore that were unrelated with vegetation cooling. For each city, the detrending process isolated residuals from a linear trend-surface regression of the NDVI at sensor location against the sensors recording over the entire city ( $T_{\text{air}} \sim \text{Lat}_{\text{cityA}} + \text{Lon}_{\text{cityA}}$ ). The residuals from the regression are the  $T_{\text{air}}$  values with regional spatial drivers of  $T_{\text{air}}$  removed and were used as detrended sensor values of  $T_{\text{air}}$  for subsequent analyses. Vegetation-derived cooling magnitude was then determined by linear regression

analysis, regressing citywide NDVI against detrended sensor  $T_{\text{air}}$  at 01:00 local time. Significant regression slopes were used as a metric of the vegetation cooling magnitude ( $^{\circ}\text{C}/\text{NDVI}$ ) and used for final analysis [9, 17]. The regression slope is a singular point of citywide Delta  $T_{\text{veg}}$  for each day of study deployment. The remaining data analysis and presentation uses the significant slope of the regression of NDVI on  $T_{\text{air}}$  as the primary metric of Delta  $T_{\text{veg}}$ .

Heat waves were defined as five continuous days where the daily mean maximum temperature is  $5^{\circ}\text{C}$  above the normal mean maximum temperature, calculated from 30 year normals derived from PRISM climate data (PRISM Climate Group, Oregon State University, <http://prism.oregonstate.edu>, created 27 September 2019) [40]. To determine the significance between heat wave and post-heat wave cooling, we conducted a bootstrap randomization procedure where each cooling magnitude was shuffled and resampled with replacement. We ran 1000 variations of resampling, thereby building a data set of heat wave cooling magnitude and post-wave cooling magnitudes. Monsoon season was determined using the pre-2009 National Weather Service definition, which begins an Arizona monsoon season following three continuous days averaging a dew point  $> 12.2^{\circ}\text{C}$  (<https://climas.arizona.edu/rgbo/rio-grande-bravo-outlook-june-2017/monsoon-2017>).

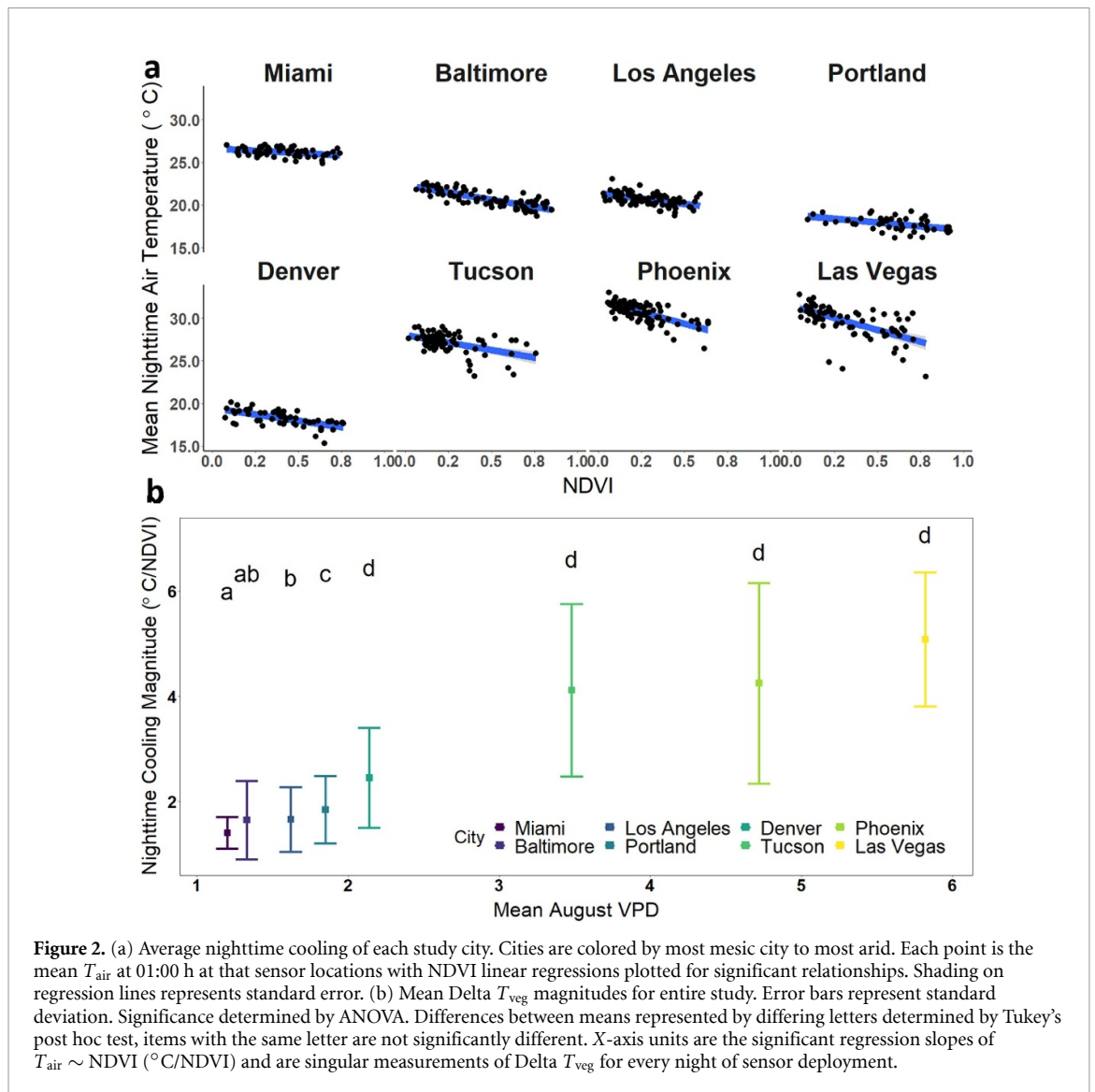


**Figure 2.** (a) Average nighttime cooling of each study city. Cities are colored by most mesic city to most arid. Each point is the mean  $T_{\text{air}}$  at 01:00 h at that sensor locations with NDVI linear regressions plotted for significant relationships. Shading on regression lines represents standard error. (b) Mean Delta  $T_{\text{veg}}$  magnitudes for entire study. Error bars represent standard deviation. Significance determined by ANOVA. Differences between means represented by differing letters determined by Tukey's post hoc test, items with the same letter are not significantly different. X-axis units are the significant regression slopes of  $T_{\text{air}} \sim \text{NDVI}$  ( $^{\circ}\text{C}/\text{NDVI}$ ) and are singular measurements of Delta  $T_{\text{veg}}$  for every night of sensor deployment.

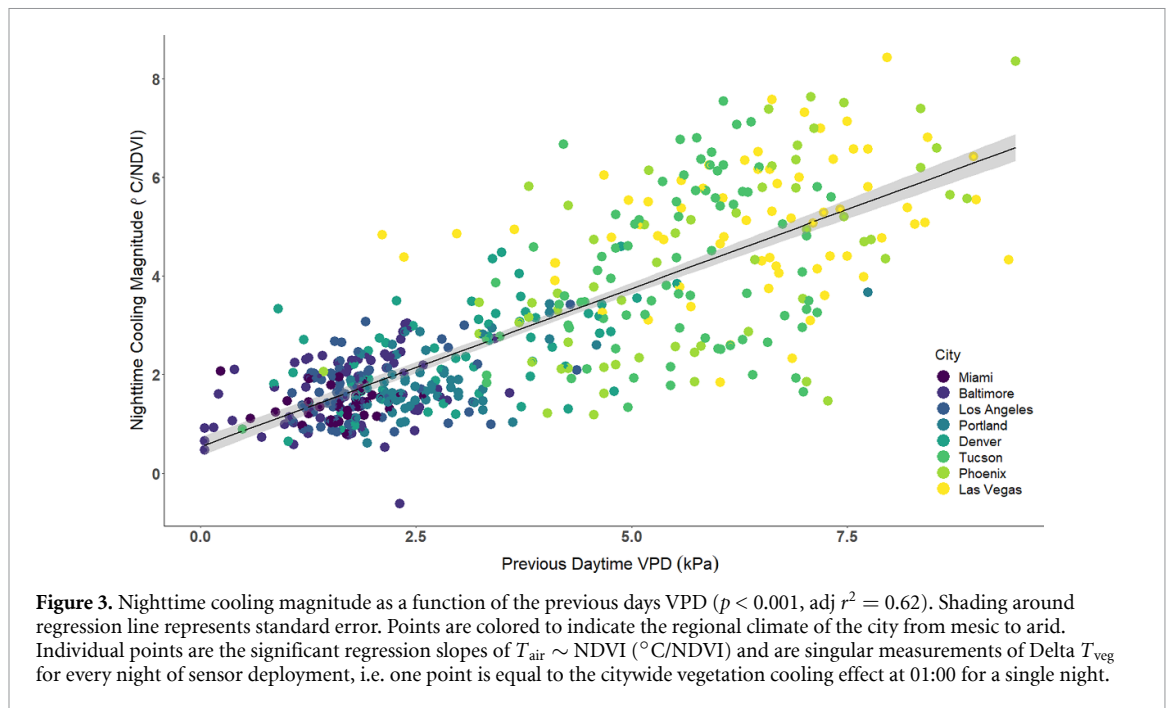
Differences between resulting slopes of the regression of site NDVI and heat-wave  $T_{\text{air}}$  of each city were determined with an analysis of variance (ANOVA) and subsequent pair-wise city differences were determined with a Tukey's post-hoc test. This method was repeated for analyzing heat waves and monsoonal effects. All statistical analyses were performed in R version 3.60 (R Core Team, 2019).

### 3. Results

Within all study cities, increased NDVI was significantly correlated with reduced nighttime  $T_{\text{air}}$  (cities ordered from least arid to most: Miami:  $p = 0.002$ ,  $r^2 = 0.14$ , Baltimore:  $p < 0.001$ ,  $r^2 = 0.63$ , Los Angeles:  $p < 0.001$ ,  $r^2 = 0.27$ , Portland:  $p < 0.001$ ,  $r^2 = 0.22$ , Denver:  $p < 0.001$ ,  $r^2 = 0.39$ , Tucson:  $p < 0.001$ ,  $r^2 = 0.23$ , Phoenix:  $p < 0.001$ ,  $r^2 = 0.48$ , Las Vegas:  $p < 0.001$ ,  $r^2 = 0.40$ ) (figure 2(a)). We computed Delta  $T_{\text{veg}}$  magnitudes as the slope of  $T_{\text{air}}$  and NDVI relationship, which generates a standardized metric of the change in air temperature

across a one-unit change in NDVI (i.e. bare ground to full vegetation). Among cities, the mean cooling magnitude varied, exhibiting a  $4.5^{\circ}\text{C}/\text{NDVI}$  range (mean slope and standard deviation of Delta  $T_{\text{veg}}$  for each city ordered from least arid to most: Miami: mean = 1.41, sd = 0.30, Baltimore: mean = 1.64, sd = 0.74, Los Angeles: mean = 1.65, sd = 0.61, Portland: mean = 1.85, sd = 0.64, Denver: mean = 2.45, sd = 0.95, Tucson: mean = 4.12, sd = 1.64, Phoenix: mean = 4.25, sd = 1.91, Las Vegas: mean = 5.08, sd = 1.27) (figure 2(b)). When comparing citywide Delta  $T_{\text{veg}}$  across the mean August VPD of each city, the mean effect of vegetation on cooling was significantly greater ( $p < 0.05$ ) in the more arid cities (i.e. Denver, Tucson, Phoenix, Las Vegas) compared to the mesic cities (i.e. Miami, Baltimore, Los Angeles, and Portland).

When comparing Delta  $T_{\text{veg}}$  to the mean mid-day VPD, calculated using dry bulb  $T_{\text{air}}$ , relative humidity, and air pressure at the local 13:00 h at the nearest airport weather station, we found significant correlation with the magnitude of



vegetation cooling the following night ( $p < 0.001$ ,  $\text{adj } r^2 = 0.62$ ) (figure 3). Yet, within each city, the midday VPD effect varied with no relationship observed in Miami or Tucson ( $p = 0.965$  and  $p = 0.237$ , respectively) (supplementary figure 1 (available online at [stacks.iop.org/ERL/16/034011/mmedia](https://stacks.iop.org/ERL/16/034011/mmedia))). Increases in ambient daytime  $T_{\text{air}}$  also increased  $\Delta T_{\text{veg}}$  across regions, and this effect was smaller than that of VPD alone ( $p < 0.001$ ,  $\text{adj } r^2 = 0.47$ ). Daytime wind-speed had no significant relationship with  $\Delta T_{\text{veg}}$  among cities, but nighttime windspeed correlated with greater air cooling; however, model fit was low ( $p < 0.001$ ,  $\text{adj } r^2 = 0.03$ ). Direct solar irradiance also had a significant positive correlation with  $\Delta T_{\text{veg}}$  magnitudes and model fit was also low ( $p < 0.001$ ,  $\text{adj } r^2 = 0.08$ ) (supplementary figure 2). A multiple linear regression of possible parameters, including VPD, direct irradiance, and nighttime windspeed had a slightly higher model fit than VPD alone ( $\text{adj } r^2 = 0.62$ ).

Temporally, the regional weather patterns differed from the mean atmospheric conditions during the study in two major ways: heat waves and seasonal monsoons. During the study, all cities experienced at least one heat wave in which the daily mean  $T_{\text{air}}$  was  $5^{\circ}\text{C}$  above the summer average for four consecutive days. Compared with the average cooling magnitude in days following heat waves,  $\Delta T_{\text{veg}}$  magnitude increased in all cities during heat waves.  $\Delta T_{\text{veg}}$  increases ranged from  $0.8^{\circ}\text{C}$  in Miami to  $3.9^{\circ}\text{C}$  in Phoenix.  $\Delta T_{\text{veg}}$  increases during heat waves also significantly scaled with the citywide mean VPD during heat waves within each city ( $p = 0.035$ ,  $\text{adj } r^2 = 0.46$ ) (figure 4(a)). Two cities (Phoenix and Tucson) experienced a shift from a dry pre-monsoon climate to a more humid monsoonal

climate. Ambient  $T_{\text{air}}$  and VPD decreased during Phoenix's monsoon season ( $T_{\text{air}}$ :  $p < 0.001$ , VPD:  $p < 0.001$ ). In Tucson, ambient  $T_{\text{air}}$  during the monsoon was consistent with pre-monsoon temperatures ( $p = 0.3$ ), but VPD decreased from pre-monsoon to monsoon season ( $p = 0.005$ ). Transitioning into the monsoon, the magnitude of vegetation cooling in Phoenix decreased from a mean of  $8.1^{\circ}\text{C}$  to  $4.6^{\circ}\text{C}$  ( $p < 0.001$ ), whereas in Tucson, the magnitude of  $\Delta T_{\text{veg}}$  decreased from a mean of  $5.0^{\circ}\text{C}$  to  $4.0^{\circ}\text{C}$  ( $p < 0.01$ ) (supplementary figure 3).

#### 4. Discussion

Increases in urban vegetation cover decrease nighttime  $T_{\text{air}}$  in cities throughout the United States; nevertheless, the magnitude of cooling varies dramatically among and within cities. Furthermore, not only was higher aridity during heat waves associated with greater cooling, but a consistent pattern also occurred in the two cities that experienced a shift between a hot and dry pre-monsoon and a more humid monsoon weather pattern. The intra-urban temporal changes in  $\Delta T_{\text{veg}}$  are consistent with the patterns observed among cities with respect to the role of daytime transpiration in nighttime cooling. Our results, spanning spatial scales of intra-urban to continental and temporal scales from individual evenings to the summer season, suggest widespread urban vegetation cooling that is consistently sensitive to aridity, implying greater latent heat fluxes in more arid cities at the same levels of vegetation coverage. The strong correlation between aridity (VPD) and the magnitude of  $\Delta T_{\text{veg}}$  is consistent with the hypothesis of transpiration as a primary influence on cooling.

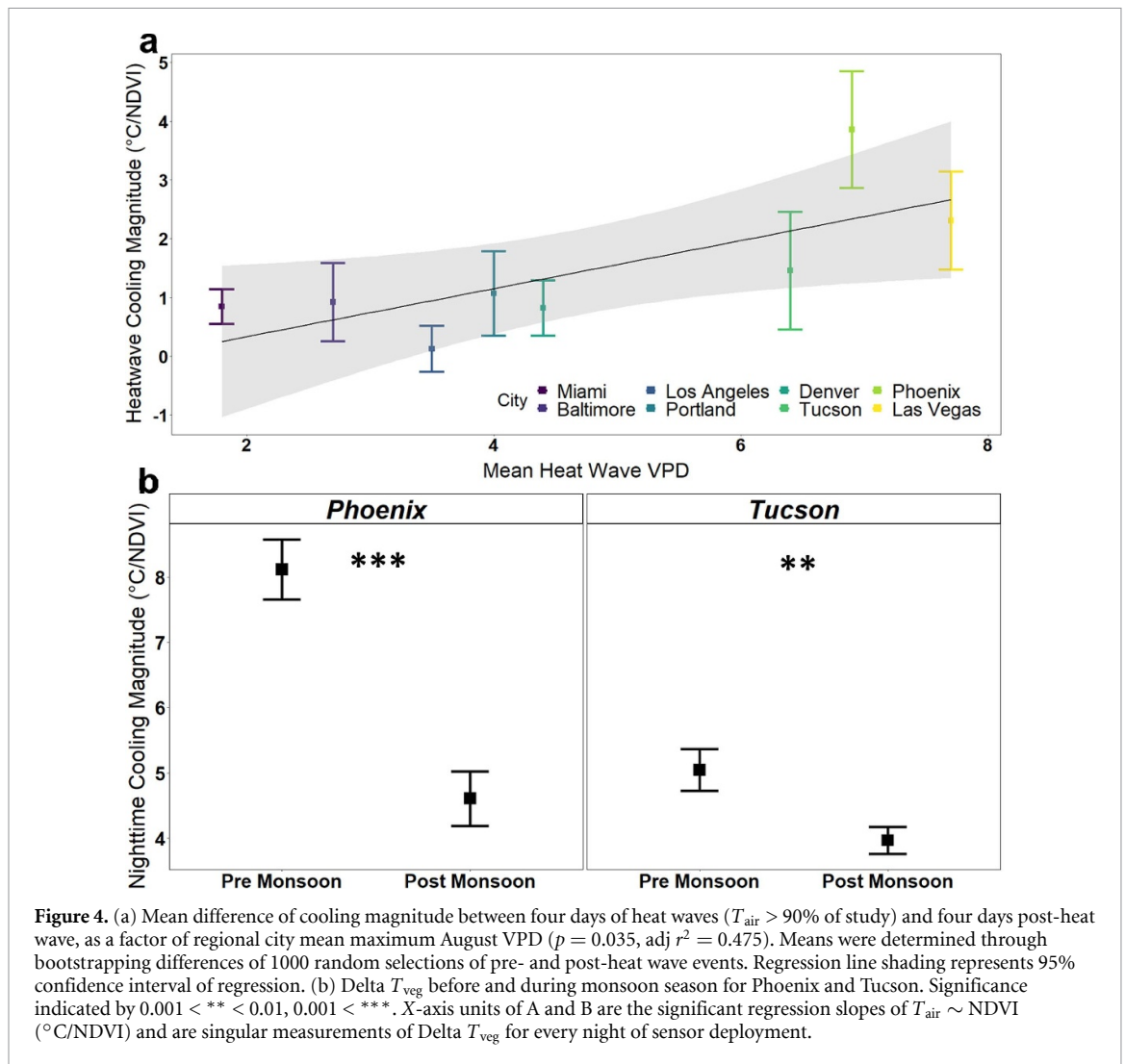


**Figure 4.** (a) Mean difference of cooling magnitude between four days of heat waves ( $T_{\text{air}} > 90\%$  of study) and four days post-heat wave, as a factor of regional city mean maximum August VPD ( $p = 0.035$ ,  $\text{adj } r^2 = 0.475$ ). Means were determined through bootstrapping differences of 1000 random selections of pre- and post-heat wave events. Regression line shading represents 95% confidence interval of regression. (b) Delta  $T_{\text{veg}}$  before and during monsoon season for Phoenix and Tucson. Significance indicated by  $0.001 < ** < 0.01$ ,  $0.001 < ***$ . X-axis units of A and B are the significant regression slopes of  $T_{\text{air}} \sim \text{NDVI}$  ( $^{\circ}\text{C}/\text{NDVI}$ ) and are singular measurements of Delta  $T_{\text{veg}}$  for every night of sensor deployment.

The dependence of Delta  $T_{\text{veg}}$  on VPD helps reconcile the large variation observed in the magnitude of vegetation cooling observed in modeling studies, surface temperature observations, and  $T_{\text{air}}$  measurements within individual regions. Our results provide needed validation that explains differences in vegetation cooling among cities using regional climate [41, 42] and microclimate [43] models that show varying cooling effects among cities and within neighborhoods. Similarly, our results indicating a strong influence of VPD on Delta  $T_{\text{veg}}$  are consistent with evaluations of satellite-derived land surface temperatures [16, 44], which also show increased daytime surface cooling in more arid conditions. Importantly, these findings suggest the large variation in observed vegetation cooling effects on urban nighttime  $T_{\text{air}}$  in varying climates may reflect a consistent underlying cause. Recent work quantifying  $T_{\text{air}}$  over vegetation gradients within individual cities reported a mean Delta  $T_{\text{veg}}$  magnitude of 5.9  $^{\circ}\text{C}$  in Palm Springs, CA [17], 3.1  $^{\circ}\text{C}$  in Los Angeles, CA [9], and a Delta  $T_{\text{veg}}$  range of 0.5  $^{\circ}\text{C}$ –1.1  $^{\circ}\text{C}$  in Madison, WI [19]. When factoring the mean summertime VPD of Palm Springs, Los Angeles, and Madison into our

results (5.4 kPa, 1.8 kPa, and 1.28 kPa respectively), we find these cooling magnitudes consistent with the results presented here that indicate a linear trend of Delta  $T_{\text{veg}}$  in response to aridity. This linear relationship between VPD with Delta  $T_{\text{veg}}$  provides a coherent transpiration-based hypothesis for extending studies within individual regions, satellite observations, and modeling approaches.

#### 4.1. Atmospheric drivers of vegetation-derived nighttime cooling

The transpiration hypothesis for regulating Delta  $T_{\text{veg}}$  suggests the importance of physiological interactions between vegetation and the urban environment. Not only is VPD a key driver of transpiration, but it also strongly correlates with Delta  $T_{\text{veg}}$  as irrigated vegetation may maintain open stomata in high VPD conditions [27]. Vegetation stabilizes surface temperature in high heat and aridity through maintaining transpiration [45]. As daytime VPD increases, urban vegetation increases transpiration, which in addition to increasing immediate latent heat flux, reduces leaf surface temperature and eventual re-radiation of stored heat energy. The combination

of these modifications to the surface energy balance are the potential causes for our observed correlation between daytime VPD and Delta  $T_{veg}$ .

As aridity increases, plants in natural areas generally exhibit a saturating relationship between transpiration and ambient VPD [22, 46], where leaves restrict their stomatal conductance in response to atmospheric drought to limit risks of xylem cavitation. However, transpiration for urban trees is less limited by high VPD relative to their rural counterparts [27]. Transpiration rates are also dependent on local soil moisture, which is generally elevated through irrigation in cities [47, 48]. We found a linear relationship between daytime VPD and Delta  $T_{veg}$ , which implies that irrigated urban vegetation experiences fewer limitations to transpiration even in conditions with high atmospheric demand. The increased transpiration resulting from irrigated vegetating experiencing high VPD could cause cooling when combined with higher wind speeds, and our results also indicated a significant, though weak, effect of nighttime wind speed on cooling (supplementary figure 2). Wind-induced air cooling is generally caused by a thinning of the leaf boundary layer that increases latent heat flux [49]; however in practice, correlations between instantaneous wind speed and air cooling are weak [25, 50]. At the continental scale, aridity appears to be the primary driver of changes in cooling magnitudes.

In addition to among-city differences in Delta  $T_{veg}$ , within-city temporal differences in Delta  $T_{veg}$  during changing weather patterns are also consistent with a hypothesized transpiration mechanism. During heat waves, plants may maintain transpiration rates [30], thereby increasing energy lost to the latent heat of evaporation and resulting in potentially greater localized air cooling. Both Phoenix and Tucson experienced greater nighttime cooling before their monsoon periods, but the effect was highest in Phoenix. Phoenix's midday VPD and  $T_{air}$  were both significantly higher than during the monsoon. However, while Tucson's daytime VPD was higher pre-monsoon, daytime air temperature was not significantly different (supplementary figure 3), which was a trend consistent with the hypothesis that VPD is a stronger driver of transpiration derived cooling compared to air temperature alone. With continued irrigation, the strength of the cooling-VPD relationship could increase with climate change in many arid regions that are projected to become more arid [51].

#### 4.2. Using urban vegetation to reduce heat-related health risks

Our study highlights the potential benefits of urban vegetation for mitigating extreme urban heat scale across cities of dramatically different climates. The linear relationships between vegetation and air temperature in all cities (figure 2(a)) imply that adding vegetation in these cities results in a continuous

cooling effect. During periods of high heat, people require a cooler nighttime temperature to sleep and reduce stress on the body [7, 52]. Reducing summertime nighttime urban heat can reduce heat stress and the need for medical treatment due to heat-related symptoms [52, 53]. Mitigating high nighttime  $T_{air}$  is important for all urban residents; however, heat-associated health effects are unevenly distributed. In the U.S., lower income and non-white racial-ethnic groups more often live in areas with less vegetation and more impervious surfaces, which is associated with hotter temperatures [54]. Conversely, individuals with higher incomes more frequently live in areas with greater vegetation cover that they can afford to irrigate, which keeps local microclimates cooler [55, 56]. Households with higher incomes can also more readily often afford air conditioning during extreme heat conditions [57, 58]. These inequalities may be exacerbated in the future as mean nighttime air temperatures are projected to increase even more than daytime temperatures [59]. For economically- and racially-marginalized groups living in areas of minimal urban vegetation, heat risks (e.g. exposure to high nighttime  $T_{air}$ ) may lead to greater vulnerability to health impacts when no coping methods (e.g. air conditioning or denser vegetation) are available.

Municipal policies considering increasing urban vegetation to mitigate heat vulnerability should also consider key trade-offs in achieving cooling. Our results show a strong influence of aridity on the magnitude of vegetation cooling; thus, in order to maintain Delta  $T_{veg}$  as an urban ecosystem service, vegetation needs to maintain transpiration. As transpiration is highly correlated to soil moisture, and irrigation practices in many cities determine soil moisture, maintaining Delta  $T_{veg}$  highlights a trade-off between cooling services and urban water use [16, 60]. The magnitude of Delta  $T_{veg}$  and expected corresponding transpiration rates are highest in cities where municipal water use concerns are of high priority. Poorly planned and extensive tree planting campaigns in arid cities may exacerbate local water shortages through increasing irrigation costs [61]. The water-for-cooling trade-off does have potential for mitigation through adaptive urban management policies of refocusing irrigation and promoting more water-conservative vegetation. In Phoenix, modeling assessments suggest nighttime air cooling could be increased with only a 2.6% water increase by shifting irrigation from areas of dense vegetation to those with sparse vegetation coverages [62]. The trade-off between air-cooling and urban water use can also be lessened by shifting vegetated landcover from primarily turf to trees and shrubs that are adapted to the local climate. For example, in the arid climate of southern Israel, the cooling efficiency of trees with no surrounding grass is 27.5 times higher than exposed turf [63].

Addressing the cost-benefit of implementing urban heat-risk management is a key goal of urban sustainability solutions [40]. Directed urban greening projects also need to be developed for specific cities. Based on our results, greening a downtown block in Baltimore ( $\sim$ NDVI = 0.09) so it resembles more of a tree-lined residential street next to a park ( $\sim$ NDVI = 0.46) would reduce nighttime air temperature by approximately 0.60 °C. The same greening program in Phoenix would result in approximately 1.3 °C of cooling. The scaling of cooling is city-specific, but discrete increases in urban greening can result in significant nighttime cooling benefits depending on the aridity of the city. Partitioning the relative cooling potentials of vegetation types beyond the total greenness metric of NDVI, in both arid and mesic cities, is a necessary next step in resolving the nexus of urban vegetation, water use, and cooling benefits. Using NDVI as a greenness metric allowed this study to compare vegetation broadly across multiple cities addressing a gap in the research of studies examining the within and among city variation in vegetation derived cooling. While some research has begun partitioning out the amount of cooling provided through shade and transpiration of urban trees [64], identifying cooling rates for different types of urban vegetated parcels [65], or modeling the potential cooling benefits of lawns and trees in a city [18], a multi-city empirical study of vegetation cooling effects delineated by vegetation type should be the next research gap addressed. Future studies should explore other covarying mechanisms of  $T_{veg}$  such as the interactions of urban vegetation, albedo, and other reductions in radiant temperature through shading. Albedo can have a significant negative correlation with nighttime surface temperature [15], and urban trees directly reduce surface temperatures through reducing incoming radiation [66]. Land surface cooling is a key component of urban heat health issues, and while out of the purview of this study of air temperatures it should not be ignored in future urban heat mitigation plants.

Our results emphasize the need for city-specific plans focused on urban vegetation as a tool to mitigate high temperatures and region-specific water limitations. Policies must be city-specific, as we have seen that increasing greening by the same amount in Las Vegas and Miami will result in significantly more cooling benefits and subsequent health benefits in arid Las Vegas. Urban stakeholders across regions can use our results to identify areas that would likely receive the most cooling benefit from increases in vegetation, especially as the negative health effects caused by urban heat are not equally distributed. Many cities have developed large scale urban forestry projects [67, 68], but without directing greening initiatives to certain areas of cities, there may be overall increases in cooling that do not address urban heat inequities. To directly address the inequity of urban

heat, rather than to focus on large city-wide greening efforts, policy makers should consider focusing urban greening to areas with the least amount of existing vegetation while also minimizing gentrification and displacement [69, 70]. As people continue to move to cities, using urban vegetation to reduce inequities in heat exposure can contribute to a more sustainable future.

### Data availability statement

The data that support the findings of this study are openly available at the following URL/DOI: [http://erams.com/s/nsR7qpFiEqUsBhm2quqZg/Urban\\_Veg\\_Cooling](http://erams.com/s/nsR7qpFiEqUsBhm2quqZg/Urban_Veg_Cooling).

### Acknowledgments

We greatly appreciate the logistical and organizational support from the Urban Water Innovation Network, especially including Mazdak Arabi and Sarah Millonig. We thank Dion Kucera, Julie Ripplinger, Holly Andrews, Mia Rochford, Samuel Meltzer, Ariane Middel, Ales Urban, Erin Everton, and Tess Gallagher for field assistance. We thank Steven Crum for helpful comments on the development of the analysis, and Janet Franklin and Louis Santiago for comments on an earlier draft of this paper. We acknowledge funding from the US National Science Foundation (CBET-1444758 and CNH-1924288).

### ORCID iDs

Peter C Ibsen  <https://orcid.org/0000-0002-3436-9100>

David M Hondula  <https://orcid.org/0000-0003-2465-2671>

Michelle L Talal  <https://orcid.org/0000-0002-1159-9974>

### References

- [1] Zhang P, Bounoua L, Imhoff M L, Wolfe R E and Thome K 2014 Comparison of MODIS land surface temperature and air temperature over the continental USA meteorological stations *Can. J. Remote Sens.* **40** 110–22
- [2] Hondula D M, Balling R C, Vanos J K and Georgescu M 2015 Rising temperatures, human health, and the role of adaptation *Curr. Clim. Change Rep.* **1** 144–54
- [3] Laaidi K, Zeghnoun A, Dousset B, Bretin P, Vandentorren S, Giraudet E and Beaudreau P 2012 The impact of heat islands on mortality in Paris during the August 2003 Heat Wave *Environ. Health Perspect.* **120** 254–9
- [4] Brooke Anderson G and Bell M L 2011 Heat waves in the United States: mortality risk during heat waves and effect modification by heat wave characteristics in 43 US communities *Environ. Health Perspect.* **119** 210–8
- [5] Johnson H, Kovats R S, McGregor G, Stedman J, Gibbs M and Walton H 2005 The impact of the 2003 heatwave on daily mortality in England and Wales and the use of rapid weekly mortality estimates *Eurosurveillance* **10** 168–71
- [6] Oke T R 1982 The energetic basis of the urban heat island *Q. J. R. Meteorol. Soc.* **108** 1–24

- [7] Chakraborty T, Hsu A, Manya D and Sheriff G 2019 Disproportionately higher exposure to urban heat in lower-income neighborhoods: a multi-city perspective *Environ. Res. Lett.* **14** 105003
- [8] Harlan S L, Brazel A J, Prasad L, Stefanov W L and Larsen L 2006 Neighborhood microclimates and vulnerability to heat stress *Soc. Sci. Med.* **63** 2847–63
- [9] Shiflett S A, Liang L L, Crum S M, Feyisa G L, Wang J and Jenerette G D 2017 Variation in the urban vegetation, surface temperature, air temperature nexus *Sci. Total Environ.* **579** 495–505
- [10] Moffett K B, Makido Y and Shandas V 2019 Urban-rural surface temperature deviation and intra-urban variations contained by an urban growth boundary *Remote Sens.* **11** 2683
- [11] Pincetl S, Prabhu S S, Gillespie T W, Jenerette G D and Pataki D E 2013 The evolution of tree nursery offerings in Los Angeles County over the last 110 years *Landscape Urban Plann.* **118** 10–17
- [12] Akbari H, Pomerantz M and Taha H 2001 Cool surfaces and shade trees to reduce energy use and improve air quality in urban areas *Sol. Energy* **70** 295–310
- [13] Taleghani M, Sailor D and Ban-Weiss G A 2016 Micrometeorological simulations to predict the impacts of heat mitigation strategies on pedestrian thermal comfort in a Los Angeles neighborhood *Environ. Res. Lett.* **11** 024003
- [14] Palta M M, Grimm N B and Groffman P M 2017 ‘Accidental’ urban wetlands: ecosystem functions in unexpected places *Front. Ecol. Environ.* **15** 248–56
- [15] Jenerette G D, Harlan S L, Buyantuev A, Stefanov W L, Declet-Barreto J, Ruddell B L, Myint S W, Kaplan S and Li X 2016 Micro-scale urban surface temperatures are related to land-cover features and residential heat related health impacts in Phoenix, AZ USA *Landscape Ecol.* **31** 745–60
- [16] Jenerette G D, Harlan S L, Stefanov W L and Martin C A 2011 Ecosystem services and urban heat riskcape moderation: water, green spaces, and social inequality in Phoenix, USA *Ecol. Appl.* **21** 2637–51
- [17] Crum S M, Shiflett S A and Jenerette G D 2017 The influence of vegetation, mesoclimate and meteorology on urban atmospheric microclimates across a coastal to desert climate gradient *J. Environ. Manage.* **200** 295–303
- [18] Wang Z-H, Zhao X, Yang J and Song J 2016 Cooling and energy saving potentials of shade trees and urban lawns in a desert city *Appl. Energy* **161** 437–44
- [19] Ziter C D, Pedersen E J, Kucharik C J and Turner M G 2019 Scale-dependent interactions between tree canopy cover and impervious surfaces reduce daytime urban heat during summer *Proc. Natl Acad. Sci. USA.* **116** 7575–80
- [20] Gómez-Navarro C, Pataki D E, Pardyjak E R and Bowling D R 2021 Effects of vegetation on the spatial and temporal variation of microclimate in the urbanized Salt Lake Valley *Agric. For. Meteorol.* **296** 108211
- [21] Wang C, Wang Z and Yang J 2018 Cooling effect of urban trees on the built environment of contiguous United States *Earth's Future* **6** 1066–81
- [22] Pataki D E, Carreiro M M, Cherrier J, Grulke N E, Jennings V, Pincetl S, Pouyat R V, Whitlow T H and Zipperer W C 2011 Coupling biogeochemical cycles in urban environments: ecosystem services, green solutions, and misconceptions *Front. Ecol. Environ.* **9** 27–36
- [23] Rahman M A, Armson D and Ennos A R 2015 A comparison of the growth and cooling effectiveness of five commonly planted urban tree species *Urban Ecosyst.* **18** 371–89
- [24] Arnfield A J 2003 Two decades of urban climate research: a review of turbulence, exchanges of energy and water, and the urban heat island *Int. J. Climatol.* **23** 1–26
- [25] Kjelgren R and Montague T 1998 Urban tree transpiration over turf and asphalt surfaces *Atmos. Environ.* **32** 35–41
- [26] Ballinas M and Barradas V L 2016 Transpiration and stomatal conductance as potential mechanisms to mitigate the heat load in Mexico City *Urban For. Urban Green* **20** 152–9
- [27] Winbourne J B, Jones T S, Garvey S M, Harrison J L, Wang L, Li D, Templer P H and Hutya L R 2020 Tree transpiration and urban temperatures: current understanding, implications, and future research directions *Bioscience* **70** 576–88
- [28] Litvak E, McCarthy H R and Pataki D E 2012 Transpiration sensitivity of urban trees in a semi-arid climate is constrained by xylem vulnerability to cavitation *Tree Physiol.* **32** 373–88
- [29] Yuan W, Zheng Y, Piao S, Ciais P and Lombardozzi D 2019 Increased atmospheric vapor pressure deficit reduces global vegetation growth *Sci. Adv.* **5** 1–14
- [30] Drake J E et al 2018 Trees tolerate an extreme heatwave via sustained transpirational cooling and increased leaf thermal tolerance *Glob Change Biol.* **24** 2390–402
- [31] Sulman B N, Roman D T, Yi K, Wang L, Phillips R P and Novick K A 2016 High atmospheric demand for water can limit forest carbon uptake and transpiration as severely as dry soil *Geophys. Res. Lett.* **43** 9686–95
- [32] Litvak E, McCarthy H R and Pataki D E 2017 A method for estimating transpiration of irrigated urban trees in California *Landscape Urban Plann.* **158** 48–61
- [33] Lindén J, Fonti P and Esper J 2016 Temporal variations in microclimate cooling induced by urban trees in Mainz, Germany *Urban For. Urban Green* **20** 198–209
- [34] Konarska J, Uddling J, Holmer B, Lutz M, Lindberg F, Pleijel H and Thorsson S 2016 Transpiration of urban trees and its cooling effect in a high latitude city *Int. J. Biometeorol.* **60** 159–72
- [35] Tucker C J 1979 Red and photographic infrared linear combinations for monitoring vegetation *Remote Sens. Environ.* **8** 127–50
- [36] Meineke E, Youngsteadt E, Dunn R R, Frank S D, Rr D and Sd F 2016 Urban warming reduces aboveground carbon storage *Proceedings of the Royal Society B: Biological Sciences* **283** 20161574
- [37] Scott A A, Zaitchik B, Waugh D W and O’Meara K 2017 Intraurban temperature variability in Baltimore *J. Appl. Meteorol. Climatol.* **56** 159–71
- [38] Crum S M and Jenerette G D 2017 Microclimate variation among urban land covers: the importance of vertical and horizontal structure in air and land surface temperature relationships 2017 *J. Appl. Meteorol. Climatol.* **56** 2531–43
- [39] Buja K and Menza C 2009 Manual for the sampling design tool for ArcGIS NOAA’s Biogeography Branch (available at: <https://www.semanticscholar.org/paper/Manual-for-the-Sampling-Design-Tool-for-ArcGIS-Buja-Menza/57d98e8ea520bb65257deae607dfa18c5de6e0ac/citing-papers>)
- [40] Georgescu M, Chow W T L, Wang Z H, Brazel A, Trapido-Lurie B, Roth M and Benson-Lira V 2015 Prioritizing urban sustainability solutions: coordinated approaches must incorporate scale-dependent built environment induced effects *Environ. Res. Lett.* **10** 061001
- [41] Georgescu M, Morefield P E, Bierwagen B G and Weaver C P 2014 Urban adaptation can roll back warming of emerging megapolitan regions *Proc. Natl Acad. Sci.* **111** 2909–14
- [42] Krayenhoff E S, Moustauoui M, Broadbent A M, Gupta V and Georgescu M 2018 Diurnal interaction between urban expansion, climate change and adaptation in US cities *Nat. Clim. Change* **8** 1097–103
- [43] Middel A, Häb K, Brazel A J, Martin C A and Guhathakurta S 2014 Impact of urban form and design on mid-afternoon microclimate in phoenix local climate zones *Landscape Urban Plann.* **122** 16–28
- [44] Zhou W, Wang J and Cadenasso M L 2017 Effects of the spatial configuration of trees on urban heat mitigation: a comparative study *Remote Sens. Environ.* **195** 1–12
- [45] Leuzinger S, Vogt R and Körner C 2010 Tree surface temperature in an urban environment *Agric. For. Meteorol.* **150** 56–62

- [46] Chen L, Zhang Z and Ewers B E 2012 Urban tree species show the same hydraulic response to vapor pressure deficit across varying tree size and environmental conditions. St. Clair S, editor *PLoS One* **7** e47882
- [47] Litvak E, Manago K, Hogue T and Pataki D E 2017 Evapotranspiration of urban landscapes in Los Angeles, California at the municipal scale *Water Resources Research* **53** 5375–7
- [48] Hochberg U, Rockwell F E, Holbrook N M and Cochard H Iso/anisohydry: a plant–environment interaction rather than a simple hydraulic trait 2018 *Trends Plant Sci.* **23** 112–20
- [49] Wolf A, Anderegg W R L and Pacala S W 2016 Optimal stomatal behavior with competition for water and risk of hydraulic impairment *Proc. Natl Acad. Sci.* **113** E7222–30
- [50] Leuzinger S and Körner C 2007 Tree species diversity affects canopy leaf temperatures in a mature temperate forest *Agric. For. Meteorol.* **146** 29–37
- [51] Overpeck J T and Udall B 2020 Climate change and the aridification of North America *Proc. Natl Acad. Sci.* **117** 11856–8
- [52] Luther M, Gardiner F W, Hansen C and Caldicott D 2016 Hot of not: physiological versus meteorological heatwaves—support for a mean temperature threshold *Int. J. Environ. Res. Public Health* **13** 3–15
- [53] Petitti D B, Hondula D M, Yang S, Harlan S L and Chowell G 2016 Multiple trigger points for quantifying heat-health impacts: new evidence from a hot climate *Environ. Health Perspect.* **124** 176–83
- [54] Nesbitt L, Meitner M J, Girling C, Sheppard S R J and Lu Y 2019 Who has access to urban vegetation? A spatial analysis of distributional green equity in 10 US cities *Landscape Urban Plann.* **181** 51–79
- [55] Tayyebi A and Darrel Jenerette G 2016 Increases in the climate change adaptation effectiveness and availability of vegetation across a coastal to desert climate gradient in metropolitan Los Angeles, CA, USA *Sci. Total Environ.* **548–549** 60–71
- [56] Hope D *et al* 2008 Socioeconomics drive urban plant diversity *Urban Ecology* (Boston, MA: Springer) pp 339–47 ([https://doi.org/10.1007/978-0-387-73412-5\\_21](https://doi.org/10.1007/978-0-387-73412-5_21))
- [57] O'Neill M S, Zanobetti A and Schwartz J 2005 Disparities by race in heat-related mortality in four US cities: the role of air conditioning prevalence *J. Urban Health* **82** 191–7
- [58] Kurn D M, Bretz S E and Akbari H 1994 The potential for reducing urban air temperatures and energy consumption through vegetative cooling sources of moisture in urban areas *Lawrence Berkeley National Lab* **4** 155–66
- [59] Donat M G and Alexander L V 2012 The shifting probability distribution of global daytime and night-time temperatures *Geophys. Res. Lett.* **39** 1–5
- [60] Ellison D *et al* 2017 Trees, forests and water: cool insights for a hot world *Glob Environ Change* **43** 51–61
- [61] Roman L A, Conway T M, Eisenman T S, Koeser A K, Ordóñez Barona C, Locke D H, Jenerette G D, Östberg J and Vogt J 2020 Beyond 'trees are good': disservices, management costs, and tradeoffs in urban forestry *Ambio* (<https://doi.org/10.1007/s13280-020-01396-8>)
- [62] Gober P, Brazel A, Quay R, Myint S, Grossman-Clarke S, Miller A and Rossi S 2010 Using watered landscapes to manipulate urban heat island effects: how much water will it take to cool phoenix? *J. Am. Plan. Assoc.* **76** 109–21
- [63] Shashua-Bar L, Pearlmutter D and Erell E 2009 The cooling efficiency of urban landscape strategies in a hot dry climate *Landscape Urban Plann.* **92** 179–86
- [64] Rahman M A, Moser A, Gold A, Rötzer T and Pauleit S 2018 Vertical air temperature gradients under the shade of two contrasting urban tree species during different types of summer days *Sci. Total Environ.* **633** 100–11
- [65] Konarska J, Holmer B, Lindberg F and Thorsson S 2016 Influence of vegetation and building geometry on the spatial variations of air temperature and cooling rates in a high-latitude city *Int. J. Climatol.* **36** 2379–95
- [66] Thom J K, Coutts A M, Broadbent A M and Tapper N J 2016 The influence of increasing tree cover on mean radiant temperature across a mixed development suburb in Adelaide, Australia *Urban For. Urban Green* **20** 233–42
- [67] Pincetl S, Gillespie T, Pataki D E, Saatchi S and Saphores J D 2013 Urban tree planting programs, function or fashion? Los Angeles and urban tree planting campaigns *GeoJournal* **78** 475–93
- [68] McPhearson P T, Feller M, Felson A, Karty R, Lu J W T, Palmer M I and Wenskus T 2010 Assessing the effects of the urban forest restoration effort of millontreesnyc on the structure and functioning of New York City ecosystems *Cities Environ.* **3** 1–21
- [69] Wolch J R, Byrne J and Newell J P 2014 Urban green space, public health, and environmental justice: the challenge of making cities 'just green enough' *Landscape Urban Plann.* **125** 234–44
- [70] Goodling E, Green J and McClintock N 2015 Uneven development of the sustainable city: shifting capital in Portland, Oregon *Urban Geogr.* **36** 504–27